# Imidazoquinoline Derivatives as Potential Inhibitors of InhA Enzyme and Mycobacterium tuberculosis

Pascal Hoffmann, Joëlle Azéma-Despeyroux, Fernanda Goncalves, Alessandro Stamilla, Nathalie Saffon-Merceron, Frédéric Rodriguez, Giulia Degiacomi, Maria Rosalia Pasca, Christian Lherbet

*Article*

# Imidazoquinoline derivatives as potential inhibitors of InhA enzyme and *Mycobacterium tuberculosis*

**Pascal Hoffmann, [1] Joëlle Azéma-Despeyroux, [1] Fernanda Goncalves, [1] Alessandro Stamilla, [2] Nathalie Saffon-Merceron, [3] Frédéric Rodriguez, [1] Giulia Degiacomi, [2] Maria Rosalia Pasca [2] and Christian Lherbet [1,*]**

[1] Laboratoire de Synthèse et Physico-Chimie de Molécules d'Intérêt Biologique (SPCMIB), - UMR5068, CNRS, Université Paul Sabatier-Toulouse III, France; pascal.hoffmann@univ-tlse3.fr; joelle.azema-despeyroux@univ-tlse3.fr; fernanda.goncalves@cnrs.fr; christian.lherbet@univ-tlse3.fr
[2] Department of Biology and Biotechnology "Lazzaro Spallanzani", University of Pavia, Pavia, Italy; alessandro.stamilla@unipv.it; giulia.degiacomi@unipv.it; mariarosalia.pasca@unipv.it
[3] Institut de Chimie de Toulouse, ICT-UAR2599, Université Toulouse III Paul Sabatier, Toulouse, France; nathalie.saffon@univ-tlse3.fr
* Correspondence: christian.lherbet@univ-tlse3.fr

**Abstract:** Tuberculosis is a serious public health problem worldwide. The search for new antibiotics has become a priority, especially with the emergence of resistant strains. A new family of imidazoquinoline derivatives, structurally analogous to triazolophthalazines, which had previously shown good antituberculosis activity, were designed to inhibit InhA, an essential enzyme for Mycobacterium tuberculosis survival and Mycobacterium tuberculosis. Over twenty molecules were synthesized and the results showed modest inhibitory efficacy against the protein. Docking experiments were carried out to show how these molecules could interact to the protein's substrate binding site. Disappointingly, unlike triazolophthlazines, these imidazoquinoline derivatives showed an absence of inhibition on mycobacterial growth.

**Keywords:** Mycobacterium tuberculosis, InhA enzyme, inhibitor, Imidazoquinoline, triazolophthalazine

## 1. Introduction

Tuberculosis (TB) is a worldwide scourge, with one third of the total world population infected by Mycobacterium tuberculosis (MTB). According to WHO report, 10 million people developed TB disease in 2021 and a total of 1.5 million died from TB [1]. Despite significant and long-term efforts, tuberculosis represents an ongoing public health threat. Drug resistance could be observed and especially multidrug resistance (MDR). MDR tuberculosis is a form cause by mycobacteria that did not respond to the most used first-line drugs i.e. Isoniazid (INH) and rifampicin. The discovery of new drugs becomes a necessity and represents a challenge for the scientific community. Fortunately, new drugs have appeared on the market in recent years, such as bedaquiline [2] and nitroimidazoles pretomanid [3] and delamanid [4], for which resistances are already emerging. Other promising drugs such as PBTZ169, TBA7371, potent inhibitors of decaprenylphosphoryl-β-D-ribose 2′-epimerase or Q203, an inhibitor with high specificity for the cytochrome bc1 complex are in clinical trials. Despite these apparent progresses, there is an urgent need for new anti-TB drugs.

Enzymes belonging to the FAS-II system required for the biosynthesis of mycolic acids, represent promising targets for the discovery of new anti-TB drugs. Among them, the enoyl ACP-reductase InhA is the primary target of the first-line anti-TB drug INH. INH acts as a prodrug that requires activation by the catalase-peroxidase KatG. For

several years, resistance has been observed for INH, mainly due to resistances on KatG. So, to overcome these resistance problems, direct inhibitors of InhA, requiring no prior activation step, have been designed and shown to be promising, such as TCL derivatives [5, 6, 7, 8, 9, 10], rhodanines [11], GEQ and analogues [12, 13], pyridomycin [14, 15], and 4-hydroxy-2-pyridones [16].

We recently described the synthesis of derivatives bearing triazole scaffolds exhibiting promising anti-TB activities [17, 18, 19]. Among all derivatives investigated so far, tricyclic triazolophthalazine compounds, synthesized in a few steps, were found to be the most interesting. Indeed, a series of 3-substituted triazolophthalazines were evaluated for their antimycobacterial activities. Among them, compounds **Cpd 1a** and **Cpd 1b** have been shown to inhibit the MTB strain H37Rv with a minimum inhibitory concentration (MIC) of less than 5 μg/mL (Figure 1).

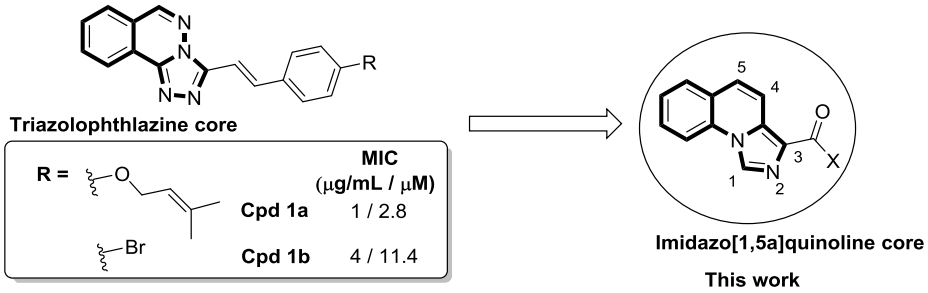


**Figure 1**. Design of imidazo[1,5-*a*]quinoline inhibitors

Based on these results, we decided to explore imidazoquinoline as isostere of the triazolophthalazine scaffold. Imidazo[1,5-a]quinoline as for triazolophthalazine is a tricyclic core found in many heterocyclic compounds that have shown several applications in medicinal and material chemistry [20]. Some of them have been designed and synthesized as neurokinin (NK1) receptor ligands [21] or highly potent ligands of central benzodiazepine receptors [22].

Therefore, we envisioned two purposes for these imidazoquinoline molecules: (1) as novel pharmacophores for InhA inhibitors; (2) as isostere scaffolds of triazolophthalazines to achieve inhibition of mycobacterial strains.

## 2. Results

### *2.1. Chemistry*

One of the limitations for the synthesis of triazolophthalazine derivatives was their low solubility, which makes chemical modifications difficult. On the other hand, functionalized Imidazoquinoline derivatives could be easily synthesized in two steps with the introduction of an ester or amide group in position 3 on imidazole. As outlined in Schemes 1 and 2, we considered the preparation of triazolophthalazine-like compounds bearing different amide groups directly bound to the heterocyclic moiety. Imidazo[1,5a]quinoline could be easily prepared by different reported methods [22, 23].

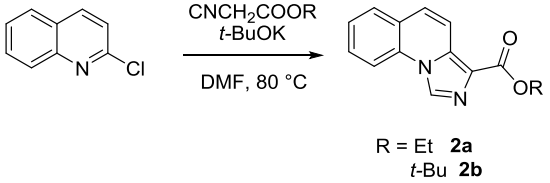


**Scheme 1**. Synthesis of esters 2a and 2b.

The general synthesis of imidazoquinoline compounds **4** is outlined in Schemes 1, 2 and 3. Esters **2a** and **2b** were synthesized in one step from commercially available 2-chloroquinoline through an imidazole-annulation with ethyl isocyanoacetate or tert-butyl isocyanoacetate in the presence of potassium tert-butoxide (Scheme 1). After hydrolysis of ester **2b** in acidic conditions, compound **3** was coupled to different cyclic and acyclic amines using the EDC•HCl/HOBt couple as coupling agent in the presence of the Hünig base DIPEA (Scheme 2). The structures of compounds **4g** and **4h** were confirmed by X-ray crystallography (Figure 2) [24].

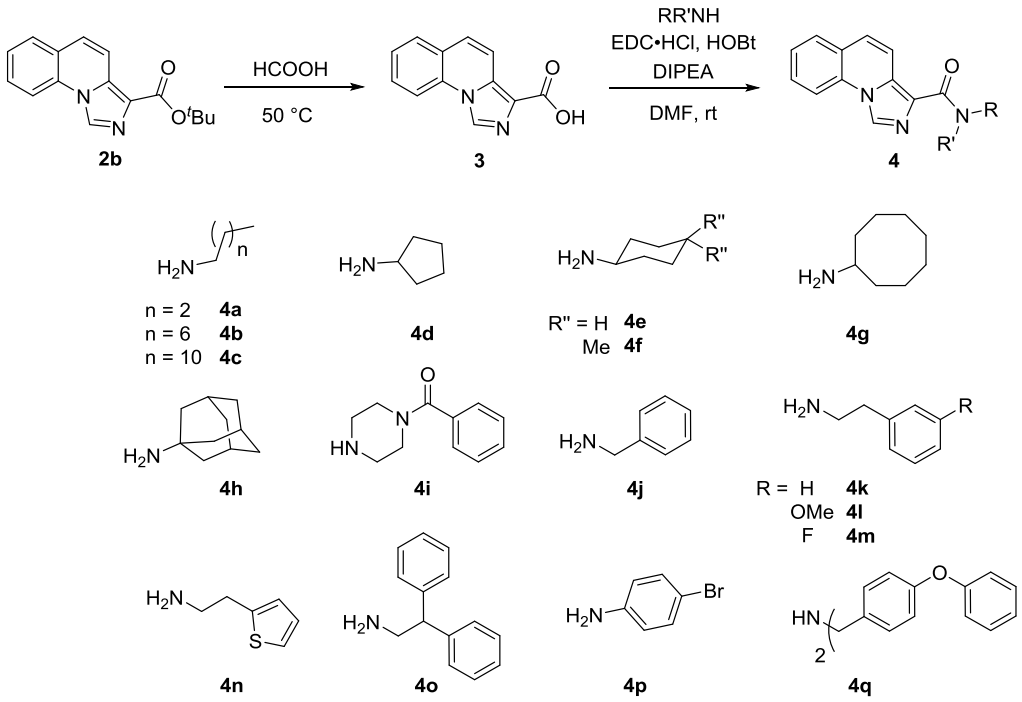


**Scheme 2**. Synthesis of amide derivatives **4a**-**4p**

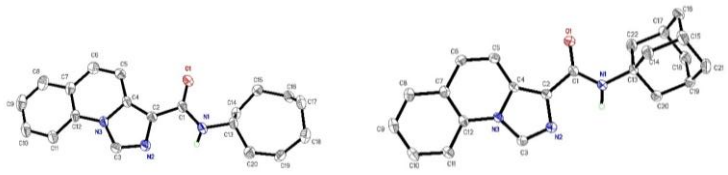

**Figure 2.** Molecular view of the X-ray crystal structures of amides **4g** (Left) and **4h** (right) (Scheme 2), with thermal ellipsoids drawn at the 30% probability level. Except for H atom on N1, hydrogen atoms were omitted for clarity.

The alkyne derivative **4r**, obtained from compound **3** and propargylamine, was further coupled to dodecyl azide by Huisgen Cu(I)-catalyzed alkyne-azide cycloaddition to afford compound **4s** in 66% yield (Scheme 3).

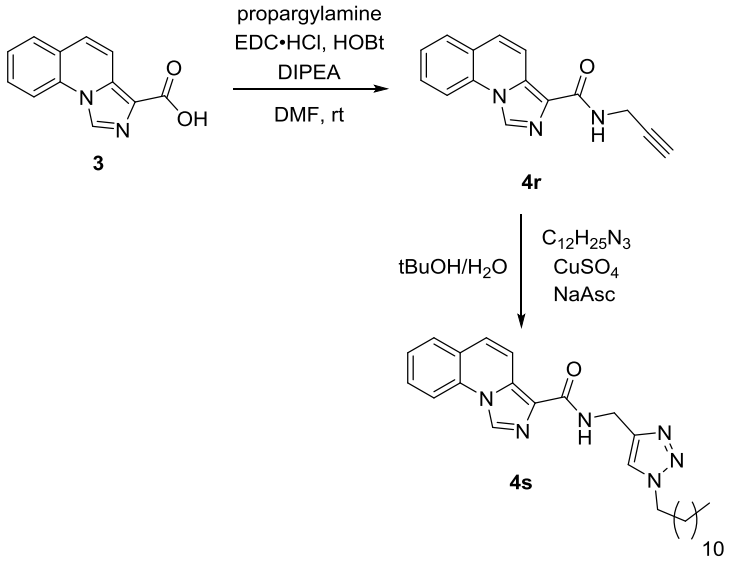


**Scheme 3.** Synthesis of amide derivatives **4r**-**4s**

*2.2. Biological activity*

*2.2.1. InhA inhibition.*

Compounds **4** were then evaluated as inhibitors of MTB InhA. These molecules can combine both the presence of hydrophobic chains that can interact with the hydrophobic pocket of InhA and an amide bond that has the potential to interact with tyrosine 158 of the protein. Triclosan was used as a control.

**Table 1.** Inhibitory activity of imidazoquinoline compounds against InhA enzyme

| Cpd | *% inhibition at 50 µM* | Purity (%) by LC-MS |
|---|---|---|
| **2a** | 26 | ND[a] |
| **2b** | 17 | ND[a] |
| **4a** | 40 | >99 |
| **4b** | 29 | >99 |
| **4c** | 16 | 98 |
| **4d** | 0 | >99 |
| **4e** | 23 | >99 |
| **4f** | 10 | >99 |
| **4g** | 19 | >99 |
| **4h** | 4 | 97 |
| **4i** | 9 | 94 |
| **4j** | 31 | >99 |
| **4k** | 13 | >99 |
| **4l** | 7 | 98 |
| **4m** | 8 | 97 |
| **4n** | 66 (24)[b] | >99 |

| | | |
|---|---|---|
| **4o** | 16 | 99 |
| **4p** | 15 | 98 |
| **4q** | 34 | 97 |
| **4r** | 49 | >99 |
| **4s** | 33 | 97 |
| **Triclosan** | 98 | **---** |

a. ND for not determined; b. Compound tested at 5 μM

Different kind of substituents on the amide group were screened in an attempt to obtain active molecules. Except for compounds **4d** (bearing a cyclopentenyl moiety), **4h** (adamantyl), **4i** (benzoylpiperazinyl), **4l** and **4m** (substituted phenethyl), which exhibit poor inhibition activity of 10% or less, all other compounds were found to significantly inhibit the enzymatic reaction at 50 μM, but with activities much lower than that obtained with triclosan. Even compound **4q**, which possesses the biarylether moiety mimicking the two molecules of triclosan able to bind in the substrate binding site of InhA, is not very active with only 34% inhibition at 50 μM. The derivatives showing the most inhibitory activity were compounds **4a** (C3-alkyl chain, 40% inhibition), **4r** (propargyl, 49% inhibition) and **4n** bearing a thiophene moiety with 66% inhibition.

*2.2.2. Inhibition of MTB growth*

The newly synthesized imidazoquinoline compounds were evaluated for their inhibitory activity against MTB H37Rv strain, using a dilution method. Minimum inhibitory concentrations (MICs) are shown in Table S1 (supporting information). Streptomycin was used as control for MTB H37Rv (MIC = 0.25 μg/mL) strain. None of them showed antimycobacterial activities below 40 μg/mL. It has to be noted that compound **4p**, analogue to **Cpd1b** (Figure 1), showed no inhibitory activity against the mycobacteria. Even compounds **4g** and **4h** structurally related to some molecules inhibiting mycobacterial membrane protein Large 3 (MmpL3) such as indole derivatives NITD-304 or NIT-349 [25, 26] were found to be not active (Figure 3). From these results it appears that the imidazoquinoline moiety seems incompatible and detrimental to good activity against mycobacterial strains.

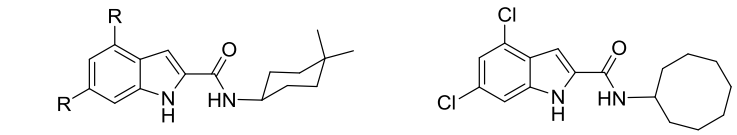


R = Cl: NITD-304, MIC (Mtb) = 0.015 μM
R = F: NITD-349, MIC (Mtb) = 0.023 μM

MIC (Mtb) = 0.0039 μM
MIC (Mtb) = 0.125 μM

**Figure 3.** Inhibitors of MmpL3.

2.3. *Docking studies*

In order to give insights on activity, docking experiments were carried out on compound **4n** that was found to have the best inhibitory activity on InhA. The best ranking docking poses (4 of the 5 first OPT protocol poses, 3 of 5 for MSE protocol, see Experimental Section for details) are those corresponding to a conformation in which the imidazoquinoline ring interacts with the nicotinamide group of $NAD^+$ through a π-stacking interaction, and is positioned towards the entry of major portal (Figure 4). These docking-poses can reasonably be considered acceptable (best poses for both protocols) according to this ligand-cofactor interaction and to the limited fluctuations of the thiophene group. It should also be noted that the position of **4n** in the substrate bind-

ing-site is comparable to that of the ligand GEQ co-crystallized in InhA (PDB entry 1P44) [13], that is, the thiophene moiety is positioned in the same way as the central five-membered cycle of the carbazole. Moreover, the tilted imidazoquinoline scaffold is positioned in the same place as the indole part of the GEQ. Compared to triclosan derivatives (i.e. JPL from 3FNG [27] or TCL from 1P45 [13]), it is interesting to underline that the imidazoquinoline heterocycle is in the same plane than the phenol ring of these TCL-ligands, and that the nitrogen atoms are positioned in approximatively the same positions than the oxygens atoms of TCL, JPL and GEQ sharing the same hydrogen bonds with ribose of the cofactor. The interaction with the positively charged nitrogen of nicotinamide group has disappeared, but the interaction with TYR158 is maintained. A hydrogen bond is probably also formed between the nitrogen of the amide group of compound **4n** and the oxygen of the nicotinamide group of the cofactor. An additional ◎-sulfur type interaction of the thiophene group and MET155 and MET199 could also be involved.

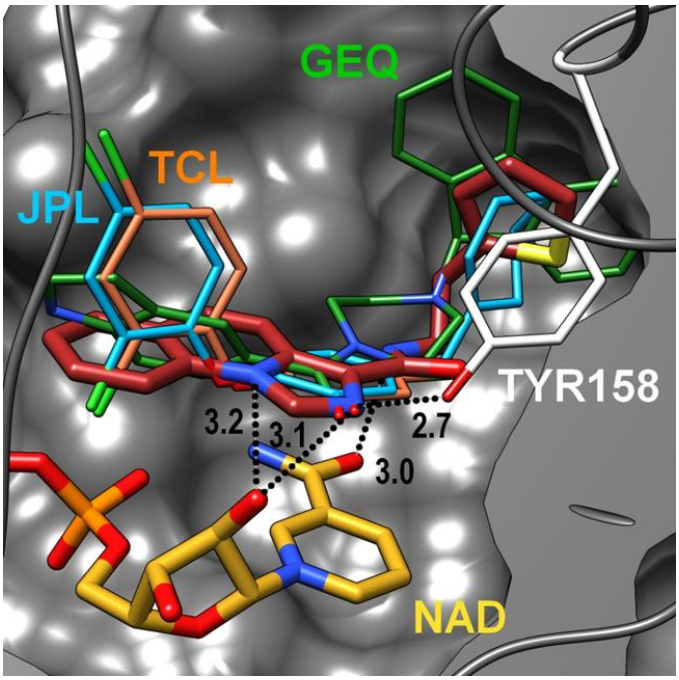


**Figure 4**. Best docked pose of compound **4n** in 1P45: A structure. The protein (ribbons and molecular surface) is depicted in grey, compound **4n** in dark red, the cofactor (NAD+, lower part) in gold, the TYR158 in white. The reference ligands are shown using small sticks, orange for TCL500 (from 1P45:B), blue for JPL (from 3FNG) and green for GEQ (from 1P44). The interatomic distances are expressed in angstroms.

## 3. Conclusions

In summary, a new series of imidazoquinoline compounds designed as potential InhA inhibitors were synthesized in good yields through a three-step procedure. These compounds were evaluated as possible inhibitors of the InhA enzyme, but disappointly were found to weakly inhibit InhA, compound 4n showing the best, but moderate, activity. Docking studies showed a possible interaction mode in the protein substrate binding site. Secondly, being isosteric analogues of triazolophthalazine derivatives and for their resemblance for MmpL3 inhibitors, they were evaluated as inhibitors of MTB strain. But these molecules showed no inhibitory activity. The introduction of various

substituents from aryl to alkyl on the amide failed to get activities against mycobacteria. Other isosteric compounds are currently being synthesized for evaluation against MTB.

## 4. **Experimental**

### *4.1. Materials and methods*

All chemicals were purchased from Aldrich-Sigma or Alfa-Aesar and used without further purification. Anhydrous solvents were freshly distilled before use or were obtained from the M. Braun Solvent Purification System (MB-SPS-800). $^{1}$H NMR spectra were recorded on a Bruker spectrometer at 300 or 500 MHz for $^{1}$H NMR experiments and at 75 or 125 MHz for $^{13}$C NMR experiments. For $^{1}$H NMR and $^{13}$C NMR, the residual solvent was used as an internal reference: $CDCl_3$ δ = 7.26 ppm, 77.0 ppm and DMSO = 2.50 ppm, 39.52 ppm. Proton coupling patterns are abbreviated as follows: s (singlet), d (doublet), t (triplet), q (quartet), and m (multiplet). Coupling constants (J) are reported in Hz. High-resolution mass spectra (HRMS) were recorded with a MAT 95XL spectrometer (ThermoFisher, Waltham, MA, USA) or on a UPLC Xevo G2 Q-TOF Waters using electrospray ionization methods. Desired products were purified by flash column chromatography with puriFlash 430 system using puriFlash® columns from Interchim.

### *4.2. Chemistry*

#### *4.2.1. General procedure for the synthesis of imidazole compounds*.

To a solution of potassium tert-butoxide (4.58 mmol, 1.5 eq) in anhydrous DMF (10 mL/mmol) at 4 °C, were added 2-chloroquinoline (0.5 g, 3.05 mmol) and isocyanoacetate (4.58 mmol, 1.5 eq). This reaction mixture was stirred for 30 min at 4 °C then 1 h at room temperature and finally 20 h at 80 °C. After cooling at room temperature, acetic acid (1 mL/mmol) was added and the mixture was stirred for 20 min. The resulting solution was poured in cooled water and the product was extracted with ethyl acetate. The organic phases were combined and were washed three times with water, dried over $MgSO_4$, filtered and concentrated under reduced pressure. The desired product was purified by flash chromatography.

Ethyl imidazo[1,5-a]quinoline-3-carboxylate (**2a**). The desired product was isolated after flash chromatography (petroleum ether/ethyl acetate 7/3 to 2/8 in 15 min) as a white powder (0.441 g, 78%). $^{1}$H NMR (300 MHz, $CDCl_3$) δ 8.51 (s, 1H); 7.89 (t, J = 7.9 Hz, 1H); 7.62 (d, J = 7.8 Hz, 1H); 7.52 (td, J = 7.8 Hz, 1.3 Hz, 1H); 7.38 (t, J = 7.6 Hz, 1.1 Hz, 1H); 7.23 (d, J = 9.5 Hz, 1H); 4.40 (q, J = 7.2 Hz, 2H); 1.40 (t, J = 7.2 Hz, 3H); $^{13}$C NMR (75 MHz, $CDCl_3$) δ 163.2; 132.4; 130.2; 129.3; 128.8; 127.8; 126.0; 125.6; 124.1; 123.8; 117.0; 114.6; 60.3; 14.4; HRMS Calculated for $C_{14}H_{13}N_2O_2$ (DCI-$CH_4$, M+H$^+$): 241.0977. Found: 241.0970.

tert-Butyl imidazo[1,5-a]quinoline-3-carboxylate (**2b**). The same protocol that those for compound 2a was used. The desired product was isolated after flash chromatography (petroleum ether/ethyl acetate 7/3 to 2/8 in 15 min) as a yellow solid upon standing (0.654 g, Yield 80%). $^{1}$H NMR (300 MHz, $CDCl_3$) δ 8.55 (s, 1H); 7.95 (d, J = 9.6 Hz, 1H); 7.93 (d, J = 8.3 Hz, 1H); 7.67 (d, J = 7.9 Hz, 1.5 Hz, 1H); 7.55 (td, J = 7.9 Hz, 1.5 Hz, 1H); 7.41 (td, J = 7.6 Hz, 1.1 Hz, 1H); 7.27 (d, J = 9.6 Hz, 1H); 1.65 (s, 9H); $^{13}$C NMR (75 MHz, $CDCl_3$) δ 162.6; 132.0; 130.3; 129.3; 128.8; 127.7; 126.0; 125.5; 125.3; 123.9; 117.5; 114.6; 81.0; 28.4; HRMS Calculated for $C_{16}H_{16}N_2O_2$ (DCI-$CH_4$, M): 268.1212. Found: 268.1208.

Imidazo[1,5-a]quinoline-3-carboxylic acid (**3**). A solution of compound **2b** (0.273 g, 3.72 mmol) in formic acid (2 mL) was stirred at 50 °C for overnight. After reaction completion

as indicated by TLC analysis, the reaction mixture was evaporated to dryness. The crude product was used in the next step without further purification

*4.2.2. General procedure for the coupling of the different amines with compound* ***3*** *(****4a-4s****).*

Typically, to a solution of compound **3** (0.070 g, 0,330 mmol) in anhydrous DMF at 4 °C, were successively added N-(3-dimethylaminopropyl)-N′-ethylcarbodiimide hydrochloride, EDC•HCl (0. 396 mmol, 1.2 eq), HOBt (0.396 mmol, 1.2 eq), amine (0.396 mmol, 1.2 eq); DIPEA (0.825 mmol, 2.5 eq). The reaction mixture was allowed to warm up to room temperature and was stirred for 20 h. Water was added and the product was extracted with ethyl acetate. The organic phases were combined and were washed three times with water, dried over $MgSO_4$, filtered and concentrated under reduced pressure. The desired product was purified by flash chromatography.

N-Butylimidazo[1,5-a]quinoline-3-carboxamide (4a). The desired product was isolated after flash chromatography (petroleum ether/ethyl acetate 7/3 to 2/8 in 15 min) as a white powder (52 mg, 57%). $R_f$ = 0.41 (petroleum ether/ethyl acetate 6/4). $^1$H NMR (300 MHz, $CDCl_3$) δ 8.50 (s, 1H); 8.20 (d, J = 9.5 Hz, 1H); 7.97 (d, J = 8.3 Hz, 1H); 7.73 (dd, J = 7.9 Hz, 1.4 Hz, 1H); 7.60 (td, J = 7.7 Hz, 1.4 Hz, 1H); 7.47 (td, J = 7.5 Hz, 1.1 Hz, 1H); 7.28 (d, J = 9.6 Hz, 1H); 7.24 (br peak, 1H); 13C NMR (75 MHz, $CDCl_3$) δ 163.3; 130.5; 130.1; 129.1; 127.2; 126.3; 126.1; 124.6; 124.3; 118.2; 114.6; 38.6; 32.0; 20.2; 13.8; HRMS Calculated for $C_{16}H_{18}N_3O$ (DCI-$CH_4$, M+H$^+$): 268.1450. Found: 268.1443. Purity (HPLC): >99% at 254 nm (tR = 2.18 min).

N-Octylimidazo[1,5-a]quinoline-3-carboxamide (**4b**). The desired product was isolated after flash chromatography (petroleum ether/ethyl acetate 8/2 to 2/8 in 15 min) as a white powder (70 mg, 70%). $R_f$ = 0.47 (petroleum ether/ethyl acetate 6/4). 1H NMR (300 MHz, $CDCl_3$) δ 8.49 (s, 1H); 8.20 (d, J = 9.4 Hz, 1H); 7.96 (d, J = 8.2 Hz, 1H); 7.72 (dd, J = 7.8 Hz, 1.2 Hz, 1H); 7.59 (td, J = 7.8 Hz, 1.3 Hz, 1H); 7.46 (td, J = 7.6 Hz, 1.1 Hz, 1H); 7.23-7.29 (m, 2H); 3.47 (q, J = 6.7 Hz, 2H); 1.64 (m, 2H); 1.20-1.52 (m, 10 H); 0.86 (t, J = 6.7 Hz, 3H); 13C NMR (75 MHz, $CDCl_3$) δ 163.3; 130.5; 130.1; 129.0; 127.2; 126.3; 126.0; 124.6; 124.3; 118.2; 114.6; 38.9; 31.8; 29.9; 29.3; 29.2; 27.0; 22.6; 14.0; HRMS Calculated for $C_{20}H_{25}N_3O$ (DCI-$CH_4$, M+H$^+$): 324.2076. Found: 324.2065. Purity (HPLC): >99% at 254 nm (tR = 4.62 min).

N-Dodecylimidazo[1,5-a]quinoline-3-carboxamide (**4c**). The desired product was isolated after flash chromatography (petroleum ether/ethyl acetate 7/3 to 2/8 in 15 min) as a white powder (92 mg, 69%). $^1$H NMR (300 MHz, $CDCl_3$) δ 8.49 (s, 1H); 8.20 (d, J = 9.7 Hz, 1H); 7.96 (d, J = 8.2 Hz, 1H); 7.73 (dd, J = 7.8 Hz, 1.4 Hz, 1H); 7.56-7.62 (m, 1H); 7.44 -749 (m, 1H); 7.28 (d, J = 9.7 Hz, 1H); 7.22-7.26 (br m, 1H); 3.47 (m, 2H); 1.65 (m, 2H); 1.24 -1.43 (m, 18H); 0.85 (t, J = 6.6 Hz, 3H); $^{13}$C NMR (75 MHz, $CDCl_3$) δ 163.3; 130.5; 130.1; 129.1; 127.2; 126.4; 126.1; 124.6; 124.3; 118.2; 114.6; 38.9; 31.9; 29.9; 29.61; 29.59; 29.57; 29.53; 29.4; 29.3; 27.0; 22.6; 14.1; HRMS Calculated for $C_{24}H_{34}N_3O$ (DCI-$CH_4$, M+H$^+$): 380.2702. Found: 380.2697. Purity (HPLC): 98% at 254 nm (tR = 9.57 min).

N-Cyclopentylimidazo[1,5-a]quinoline-3-carboxamide (**4d**). The desired product was isolated after flash chromatography (petroleum ether/ethyl acetate 8/2 to 2/8 in 15 min) as a white powder (55 mg, 60 %). $R_f$ = 0.35 (petroleum ether/ethyl acetate 6/4). $^1$H NMR (300 MHz, $CDCl_3$) δ 8.48 (s, 1H); 8.20 (d, J = 9.6 Hz, 1H); 7.96 (d, J = 8.3 Hz, 1H); 7.72 (dd, J = 7.8 Hz, 1.1 Hz, 1H); 7.59 (td, J = 7.7 Hz, 1.3Hz, 1H); 7.46 (td, J = 7.6 Hz, 1.1 Hz, 1H); 7.28 (d, J = 9.6 Hz, 1H); 7.18 (d, J = 7.3 Hz, 1H); 4.46 (m, 1H); 2.10 (m, 2h); 1.60-1.76 (m, 6H); $^{13}$C NMR (75 MHz, $CDCl_3$) δ 162.9; 130.5; 130.1; 127.2; 126.3; 126.1; 124.6; 124.3; 118.2; 114.6; 50.6;

33.3; 23.8; HRMS Calculated for $C_{17}H_{18}N_3O$ (DCI-$CH_4$, M+H$^+$): 280.1450. Found: 280.1439. Purity (HPLC): >99% at 254 nm (tR = 2.22 min).

N-Cyclohexylimidazo[1,5-a]quinoline-3-carboxamide (**4e**). The desired product was isolated after flash chromatography (petroleum ether/ethyl acetate 8/2 to 2/8 in 15 min) as a white powder (71 mg, 71%). $R_f$ = 0.45 (petroleum ether/ethyl acetate 6/4). $^1$H NMR (300 MHz, $CDCl_3$) δ 8.47 (s, 1H); 8.18 (d, J = 9.4 Hz, 1H); 7.94 (d, J = 8.4 Hz, 1H); 7.70 (dd, J = 7.9 Hz, 1.3 Hz, 1H); 7.57 (td, J = 7.8; 1.5 Hz, 1H); 7.44 (td, J = 7.6 Hz, 1.1 Hz, 1H); 7.26 (d, J = 9.4 Hz, 1H); 7.13 (d, J = 8.3 Hz, 1H); 4.00 (m, 2H); 2.04 (m, 2H); 1.75 (m, 2H); 1.63 (m, 1H); 1.15-1.50 (m, 5H); $^{13}$C NMR (75 MHz, $CDCl_3$) δ 162.4; 130.5; 130.1; 129.0; 127.3; 126.3; 126.0; 124.5; 124.3; 118.2; 114.5; 47.6; 33.3; 25.6; 25.0; HRMS Calculated for $C_{18}H_{20}N_3O$ (DCI-$CH_4$, M+H$^+$): 294.1606. Found: 294.1597. Purity (HPLC): >99% at 254 nm (tR = 2.79 min).

N-(4,4-Dimethylcyclohexyl)imidazo[1,5-a]quinoline-3-carboxamide (**4f**). The desired product was isolated after flash chromatography (petroleum ether/ethyl acetate 8/2 to 2/8 in 15 min) as a white powder (82 mg, 77%). $R_f$ = 0.59 (petroleum ether/ethyl acetate 5/5). $^1$H NMR (300 MHz, $CDCl_3$) δ 8.47 (s, 1H); 8.17 (d, J = 9.7 Hz, 1H); 7.93 (d, J = 8.3 Hz, 1H); 7.69 (dd, J = 7.8 Hz, 1.2 Hz, 1H); 7.56 (m, 1H); 7.44 (m, 1H); 7.25 (d, J = 9.5 Hz, 1H); 7.15 (d, J = 8.3 Hz, 1H); 3.95 (m, 1H); 1.89 (m, 2H); 1.30-1.57 (m, 6H); 0.94 (s, 3H); 0.93 (s, 3H); $^{13}$C NMR (75 MHz, $CDCl_3$) δ 162.6; 130.5; 130.1; 129.0; 127.2; 126.0; 124.6; 124.2; 118.1; 114.5; 47.8; 37.7; 31.6; 29.5; 28.9; 25.0; HRMS Calculated for $C_20H_{24}N_3O$ (DCI-CH4, M+H+): 322.1919. Found: 322.1917. Purity (HPLC): >99% at 254 nm (tR = 2.22 min).

N-Cyclooctylimidazo[1,5-a]quinoline-3-carboxamide (**4g**). The desired product was isolated after flash chromatography (petroleum ether/ethyl acetate 7/3 to 2/8 in 15 min) as a white powder (46 mg, 66%). Crystallization (dichloromethane). $R_f$ = 0.72 (petroleum ether/ethyl acetate 4/6). $^1$H NMR (300 MHz, $CDCl_3$) δ 8.49 (s, 1H); 8.20 (d, J = 9.5 Hz, 1H); 7.95 (d, J = 8.4 Hz, 1H); 7.71 (dd, J = 7.8 Hz, 1.2 Hz, 1H); 7.59 (td, J = 7.8 Hz, 1.5 Hz, 1H); 7.46 (td, J = 7.6 Hz, 1.2 Hz, 1H); 7.27 (d, J = 9.5 Hz, 1H); 7.21 (d, J = 8.2 Hz, 1H); 4.24 (m, 1H); 1.97 (m, 2H); 1.60 (m, 12H); 13C NMR (75 MHz, $CDCl_3$) δ 162.3; 130.5; 130.1; 129.04; 129.02; 127.3; 126.3; 126.0; 124.6; 124.3; 118.2; 114.6; 48.7; 32.5; 27.2; 25.5; 23.8; HRMS Calculated for $C_{20}H_{24}N_3O$ (DCI-$CH_4$, M+H$^+$): 322.1919. Found: 322.1906. Purity (HPLC): >99% at 254 nm (tR = 3.84 min).

N-(Adamantan-1-yl)imidazo[1,5-a]quinoline-3-carboxamide (**4h**). The desired product was isolated after flash chromatography (petroleum ether/ethyl acetate 7/3 to 2/8 in 15 min) as a white powder (47 mg, 39%). $R_f$ = 0.49 (petroleum ether/ethyl acetate 6/4). $^1$H NMR (300 MHz, $CDCl_3$) δ 8.47 (s, 1H); 8.18 (d, J = 9.6 Hz, 1H); 7.95 (d, J = 8.3 Hz, 1H); 7.71 (dd, J = 7.8 Hz, 1.3 Hz, 1H); 7.58 (td, J = 7.8 Hz, 1.5 Hz, 1H); 7.46 (td, J = 7.8 Hz, 1.2 Hz, 1H); 7.25 (d, J = 7.6 Hz, 1H); 2.20 (m, 6H); 2.13 (m, 3H); 1.68-1.78 (m, 6H); $^{13}$C NMR (75 MHz, $CDCl_3$) δ 162.8; 130.6; 129.9; 129.0; 127.9; 126.0; 124.4; 124.3; 118.3; 114.6; 51.7; 41.9; 36.4; 29.5; HRMS Calculated for $C_{22}H_{24}N_3O$ (DCI-$CH_4$, M+H$^+$): 346.1919. Found: 346.1919. Purity (HPLC): 97% at 254 nm (tR = 4.51 min).

1-Benzoyl-4-({imidazo[1,5-a]quinolin-3-yl}carbonyl)piperazine (**4i**). The desired product was isolated after flash chromatography (petroleum ether/ethyl acetate 2/8 to 100% ethyl acetate in 15 min) as a white powder (94 mg, 74%). $R_f$ = 0.27 (ethyl acetate). $^1$H NMR (300 MHz, $CDCl_3$) δ 8.53 (br s, 1 H); 8.09 (d, J = 9.5 Hz, 1H); 7.99 (d, J = 8.4 Hz, 1H); 7.74 (dd, J = 7.7 Hz, 1.1 Hz, 1H); 7.61 (m, 1H); 7.48 (m, 1H); 7.43 (br m, 5H); 7.30 (d, J = 9.5 Hz, 1H); 3.59-4.41 (m, 8H); $^{13}$C NMR (75 MHz, $CDCl_3$) δ 170.6; 163.5; 135.4; 133.0; 130.4; 129.9; 129.2; 129.0; 128.5; 127.3; 127.0; 126.2; 124.8; 124.3; 118.2; 114.6; The carbons of the piperazine ring are missing. Calculated for $C_{23}H_{21}N_4O_2$ (DCI-$CH_4$, M+H$^+$): 385.1665. Found: 385.1655. Found: 385.1655. Purity (HPLC): 94% at 254 nm (tR = 1.51 min).

N-Benzylimidazo[1,5-a]quinoline-3-carboxamide (**4j**). The desired product was isolated after flash chromatography (petroleum ether/ethyl acetate 8/2 to 2/8 in 15 min) as a white powder (81 mg, 91%). $R_f$ = 0.44 (petroleum ether/ethyl acetate 6/4). 1H NMR (300 MHz, $CDCl_3$) δ 8.47 (s, 1H); 8.23 (d, J = 9.6 Hz, 1H); 7.95 (d, J = 8.6 Hz, 1H); 7.74 (dd, J = 7.8 Hz, 1.2 Hz, 1H); 7.58-7.63 (m, 2H); 7.48 (td, J = 7.6 Hz, 1.1 Hz, 1H); 7.24-7.42 (m, 6H); 4.69 (d, J = 5.9 Hz, 2H); 13C NMR (75 MHz, $CDCl_3$) δ 163.2; 138.7; 130.5; 130.3; 128.6; 127.8; 127.3; 126.9; 126.5; 126.1; 124.8; 124.3; 118.1; 114.6; 42.9; HRMS Calculated for $C_{19}H_{16}N_3O$ (DCI-$CH_4$, M+$H^+$): 302.1293. Found: 302.1288. Purity (HPLC): >99% at 254 nm (tR = 2.36 min).

N-(2-Phenylethyl)imidazo[1,5-a]quinoline-3-carboxamide (**4k**). The desired product was isolated after flash chromatography (petroleum ether/ethyl acetate 8/2 to 2/8 in 15 min) as a white powder (88 mg, 87 %). $R_f$ = 0.36 (petroleum ether/ethyl acetate 6/4). $^1$H NMR (300 MHz, $CDCl_3$) δ 8.48 (s, 1H); 8.21 (d, J = 9.5 Hz, 1H); 7.96 (d, J = 8.3 Hz, 1H); 7.73 (dd, J = 7.8 Hz, 1.2Hz, 1H); 7.60 (td, J = 7.8 Hz, 1.5 Hz, 1H); 7.47 (td, J = 7.6 Hz, 1.2 Hz, 1H); 7.19-7.38 (m, 7H); 3.75 (m, 2H); 2.97 (t, J = 7.4 Hz, 1H); $^{13}$C NMR (75 MHz, $CDCl_3$) δ 163.3; 139.2; 130.5; 130.2; 129.1; 129.07; 128.8; 128.6; 127.0; 126.43; 126.35; 126.1; 124.8; 124.3; 118.1; 114.6; 40.3; 36.2; HRMS Calculated for $C_{19}H_{18}N_3O$ (DCI-$CH_4$, M+$H^+$): 316.1450. Found: 316.1449. Purity (HPLC): >99% at 254 nm (tR = 2.64 min).

N-[2-(3-Methoxyphenyl)ethyl]imidazo[1,5-a]quinoline-3-carboxamide (**4l**). The desired product was isolated after flash chromatography (petroleum ether/ethyl acetate 8/2 to 2/8 in 15 min) as a white powder (72 mg, 77%). $R_f$ = 0.32 (petroleum ether/ethyl acetate 4/6). $^1$H NMR (300 MHz, $CDCl_3$) δ 8.48 (s, 1H); 8.21 (d, J = 9.5 Hz, 1H); 7.96 (d, J = 8.2 Hz, 1H); 7.74 (dd, J = 7.8 Hz, 1.2 Hz, 1H); 7.61 (m, 1H); 7.48 (m, 1H); 7.36 (m, 1H); 7.32 (d, J = 9.6 Hz, 1H); 7.22 (d, J = 7.8 Hz, 1H); 6.76-6.88 (m, 3H); 3.79 (s, 3H); 3.75 (m, 2H); 2.95 (t, J = 7.4 Hz, 2H); $^{13}$C NMR (75 MHz, CDCl3) δ 163.4; 159.7; 140.8; 130.6; 130.2; 129.5; 129.1; 127.1; 126.5; 126.1; 124.8; 124.3; 121.1; 118.1; 114.6; 114.2; 112.1; 55.2; 40.2; 36.3; HRMS Calculated for $C_{21}H_{20}N_3O_2$ (DCI-$CH_4$, M+$H^+$): 346.1556. Found: 346.1562. Purity (HPLC): 98% at 254 nm (tR = 2.57 min).

N-[2-(3-Fluorophenyl)ethyl]imidazo[1,5-a]quinoline-3-carboxamide (**4m**). The desired product was isolated after flash chromatography (petroleum ether/ethyl acetate 8/2 to 2/8 in 15 min) as a white powder (98 mg, 89%). $R_f$ = 0.39 (petroleum ether/ethyl acetate 5/5). $^1$H NMR (300 MHz, $CDCl_3$) δ 8.48 (s, 1H); 8.19 (d, J = 9.6Hz, 1H); 7.95 (d, J = 8.3 Hz, 1H); 7.72 (dd, J = 7.8 Hz, 1.3 Hz, 1H); 7.59 (m, 1H); 7.47 (m, 1H); 7.37 (t broad, J = 5.9 Hz, 1H); 7.29 (d, J = 9.6 Hz, 1H); 7..2-7.30 (m, 1H); 7.04 (d, J = 7.7 Hz, 1H); 6.98 (m, 1H); 6.88-6.94 (m, 1H); 3.73 (m, 2H); 2.96 (t, J = 7.4 Hz, 2H); $^{13}$C NMR (75 MHz, $CDCl_3$) δ 163.3; 162.9 (d, J = 94.9 Hz); 141.7 (d, J = 7.2 Hz); 130.5; 130.2; 130.0 (d, J = 8.3 Hz); 129.14; 129.06; 126.8; 126.4; 126.1; 124.9; 124.4 (d, J = 2.8 Hz); 124.3; 118.0; 115.6 (d, J = 21.0 Hz); 114.6; 113.2 (J = 20.9 Hz); 40.0; 35.9 (d, J = 1.6 Hz); $^{19}$F NMR (282 MHz, $CDCl_3$) δ −113.4; HRMS Calculated for$C_{20}H_{17}N_3OF$ (DCI-$CH_4$, M+$H^+$): 334.1356. Found: 334.1348. Purity (HPLC): 97% at 254 nm (tR = 3.01 min).

N-[2-(Thiophen-2-yl)ethyl]imidazo[1,5-a]quinoline-3-carboxamide (**4n**). The desired product was isolated after flash chromatography (petroleum ether/ethyl acetate 7/3 to 2/8 in 15 min) as a brownish powder (72 mg, 68%). $^1$H NMR (300 MHz, $CDCl_3$) δ 8.47 (s, 1H); 8.19 (d, J = 9.6 Hz, 1H); 7.95 (d, J = 8.3 Hz, 1H); 7.72 (dd, J = 7.8 Hz, 1.2 Hz, 1H); 7.56-7.62 (m, 1H); 7.44-7.47 (m, 1H) ; 7.40 (br m, 1H); 7.29 (d, J = 9.6 Hz, 1H); 7.16 (dd, J = 5.0 Hz, 1.3 Hz, 1H); 6.94-6.96 (m, 1H); 6.90 (m, 1H); 3.74-3.80 (m, 2H); 3.18 (t, J = 7.0 Hz, 2H); $^{13}$C NMR (75 MHz, $CDCl_3$) δ 163.3; 141.5; 130.5; 130.3; 129.2; 129.1; 126.8; 126.5; 126.2; 125.3; 124.9; 124.3; 123.8; 118.0; 114.6; 40.4; 30.4; HRMS Calculated for $C_{18}H_{16}N_3OS$ (DCI-$CH_4$, M+$H^+$): 322.1014. Found: 322.1015. Purity (HPLC): >99% at 254 nm (tR = 2.67 min).

N-(2,2-Diphenylethyl)imidazo[1,5-a]quinoline-3-carboxamide (**4o**). The desired product was isolated after flash chromatography (petroleum ether/ethyl acetate 70/30 to 0/100 in 15 min) as a white powder (109 mg, 84%). $^{1}$H NMR (300 MHz, $CDCl_3$) δ 8.35 (s, 1H); 8.18 (d, J = 9.5 Hz, 1H); 7.85 (d, J = 8.2 Hz, 1H); 7.68 (dd, J = 7.8 Hz, 1.2 Hz, 1H); 7.51-7.57 (m, 1H); 7.43 (m, 1H); 7.19-7.33 (m, 12H); 4.39 (t, J = 8.0 Hz, 1H); 4.13-4.17 (m, 2H); 13C NMR (75 MHz, $CDCl_3$) δ 163.3; 124.1; 130.4; 130.1; 129.0; 128.9; 128.6; 128.1; 126.6; 126.0; 124.6; 124.1; 117.9; 114.5; 50.9; 43.3; HRMS Calculated for $C_{26}H_{22}N_3O$: 392.1776 (DCI-$CH_4$, M+H+). Found: 392.1772. Purity (HPLC): 99% at 254 nm (tR = 4.61 min).

N-(4-Bromophenyl)imidazo[1,5-a]quinoline-3-carboxamide (**4p**). The desired product was isolated after flash chromatography (petroleum ether/ethyl acetate 7/3 to 2/8 in 15 min) as a white powder (69 mg, 51%). $R_f$ = 0.44 (petroleum ether/ethyl acetate 6/4). $^{1}$H NMR (500 MHz, DMSO) δ 10.29 (s, 1H); 9.34 (s, 1H); 8.56 (d, J = 8.2 Hz, 1H); 8.10 (d, J = 9.5 Hz, 1H); 7.97 (dd, J = 7.9 Hz, 1.2Hz, 1H); 7.92 (d, J = 8.9 Hz, 2H); 7.77 (td, J = 8.5 Hz, 1.3 Hz, 1H); 7.59-7.62 (m, 2H); 7.51 (d, J = 8.9 Hz, 2H); $^{13}$C NMR (125 MHz, DMSO) δ 161.4; 138.5; 131.3; 130.41; 130.39; 129.8; 129.0; 126.4; 126.1; 125.7; 123.7; 116.9; 115.9; 114.8; HRMS Calculated for $C_{18}H_{13}BrN_3O$ (ESI, M+H$^+$): 366.0242. Found: 366.0238. Purity (HPLC): 98% at 254 nm (tR = 4.66 min).

N,N-Bis[(4-phenoxyphenyl)methyl]imidazo[1,5-a]quinoline-3-carboxamide (**4q**). The desired product was isolated after flash chromatography (petroleum ether/ethyl acetate 7/3 to 2/8 in 15 min) as a white powder (112 mg, 59%). $R_f$ = 0.56 (petroleum ether/ethyl acetate 5/5). $^{1}$H NMR (300 MHz, $CDCl_3$) δ 8.55 (s, 1H); 8.29 (d, J = 9.7 Hz, 1H); 7.99 (d, J = 8.2 Hz, 1H); 7.76 (dd, J = 7.8 Hz, 1.1 Hz, 1H); 7.62 (m, 1H); 7.49 (m, 1H); 7.30-7.35 (m, 9H); 7.09 (td, J = 8.5 Hz, 1.2 Hz, 2H); 6.97-7.03 (m, 8H); 5.41 (s, 2H); 4.71 (s, 2H); $^{13}$C NMR (75 MHz, $CDCl_3$) δ 164.5; 157.26; 157.18; 156.46; 156.32; 133.1; 132.8; 132.6; 130.5; 129.8 (br peak); 129.7; 129.3 (br peak); 129.1; 129.0; 128.0; 126.1; 124.5; 124.4; 123.1; 119.0 (br peak); 118.8 (br peak); 114.6; 50.3 47.5 ; HRMS Calculated for $C_{38}H_{30}N_3O_3$ (DCI-$CH_4$, M+H$^+$): 576.2287. Found: 576.2293. Purity (HPLC): 97% at 254 nm (tR = 9.14 min).

N-(Prop-2-yn-1-yl)imidazo[1,5-a]quinoline-3-carboxamide (**4r**). The desired product was isolated after flash chromatography (petroleum ether/ethyl acetate 7/3 to 2/8 in 15 min) as a white powder (92 mg, 78%). $R_f$ = 0.52 (petroleum ether/ethyl acetate 5/5). $^{1}$H NMR (300 MHz, $CDCl_3$) δ 8.52 (s, 1H); 8.18 (d, J = 9.4 Hz, 1H); 7.99 (d, J = 8.4 Hz, 1H); 7.75 (dd, J = 7.7 Hz, 1.2 Hz, 1H); 7.63 (m, 1H); 7.50 (m, 1H); 7.42 (m, 1H); 7.33 (d, J = 9.4 Hz, 1H); 4.29 (dd, J = 5.5, 2.5 Hz, 2H); 2.26 (t, J = 2.4 Hz, 1H); $^{13}$C NMR (75 MHz, $CDCl_3$) δ 163.0; 130.5; 129.3; 129.2; 126.6; 126.4; 126.2; 125.1; 124.3; 117.9; 114.7; 79.9; 71.3; 28.6; 1 carbon is missing. HRMS Calculated for $C_{15}H_{12}N_3O$ (DCI-$CH_4$, M+H$^+$): 250.0980. Found: 250.0971. Purity (HPLC): >99% at 254 nm (tR = 1.49 min).

N-[(1-Dodecyl-1H-1,2,3-triazol-4-yl)methyl]imidazo[1,5-a]quinoline-3-carboxamide (**4s**). The desired product was isolated after flash chromatography (petroleum ether/ethyl acetate 7/3 to 0/10 in 15 min) as a white powder (48 mg, 66%). $R_f$ = 0.24 (petroleum ether/ethyl acetate 3/7). $^{1}$H NMR (300 MHz, $CDCl_3$) δ 8.60 (s, 1H); 8.20 (d, J = 9.7 Hz, 1H); 8.03 (d, J = 8.2 Hz, 1H); 7.97 (t, J = 6.0 Hz, 1H); 7.76 (dd, J = 7.9 Hz, 1Hz, 1H); 7.61-7.67 (m, 2H); 7.51 (m, 1H); 7.33 (d, J = 9.6 Hz, 1H); 4.80 (d, J = 6.1 Hz, 2H); 4.33 (t, J = 7.1 Hz, 2H); 1.90 (m, 2H); 1.25 (m, 18H); 0.89 (m, 3H); $^{13}$C NMR (75 MHz, $CDCl_3$) v 163.4; 145.4; 130.5; 130.3; 129.2; 129.0; 126.8; 126.7; 126.1; 124.9; 124.2; 122.1; 117.8; 114.7; 50.3; 34.5; 31.8; 30.2; 29.5; 29.4; 29.3; 29.2; 28.9; 26.4; 22.6; 14.1; HRMS Calculated for $C_{27}H_{37}N_6O$ (DCI-$CH_4$, M+H$^+$): 461.3029. Found: 461.3039. Purity (HPLC): 97% at 254 nm (tR = 7.84 min).

*4.2.3. Purity of the compounds*

The analysis were performed using Waters UPLC PDA SQD Simple Quadrupole Mass Spectrometer. For LC separation, chromatographic column was a BEH C18 column (100 mm × 2.1 mm, 1.7 μm, Waters); the mobile phase was consisted of water (containing 0.1% formic acid) (A) and acetonitrile (containing 0.1% formic acid) (B) with a gradient elution at a flow rate of 0.3 mL/min; The gradient elution was set as follows: 0 min, 50% B; 1 min, 50% B; 11 min, 100% B; 12 min, 100% B; 13 min, 50% B. The column temperature was 40°C. MS responses of target analytes were evaluated by electrospray ionization (ESI) in positive ion mode. Nitrogen was used as the nebulizing. The instrument settings were as follows: capillary voltage: 2.5 kV; cone voltage: 20V; de-solvent gas flow: 900 L/h; cone gas flow: 50 L/h; ion source temperature: 150 °C; Solvent temperature: 450 °C. All final compounds had a purity greater than 94% as determined by LCMS analysis.

### *4.3. Molecular docking studies of compound **4n***

#### *4.3.1. Molecular graphics*

Molecular graphics were performed with the UCSF Chimera package [28]. Chimera is developed by the Ressource for Biocomputing, Visualization, and Informatics at the University of California, San Francisco (supported by the NIGMS P41-GM103311). The protein structures used in this paper were downloaded from the RCSB Protein Database [29] and aligned [30] on a reference structure 1BVR (chain A, formerly 1BVR:A) [31]. The protein structures, were prepared (structure checks, rotamers, hydrogenation, splitting of chains) using Biovia (www.3dsbiovia.com) Discovery Studio Visualizer 2021 (DSV), UCSF Chimera and in-house Python codes. The new compounds were sketched using ChemAxon Marvin 16 (www.chemaxon.com). All ligands were checked (hybridization, hydrogenation, some geometry optimizations, 3D sketching) and merged in SDF libraries using DSV or in-house programs.

#### *4.3.2. Molecular docking*

Molecular modeling studies were carried with Molegro Virtual Docker 6 (www.molexus.com) software using aligned 1P45 (chain A, formerly 1P45:A) [13] PDB structure, that is characterized by a binding site widely opened at the major portal side and a closed minor portal.

Two molecular docking protocols (MSE, OPT) and two internal scoring schemes (Moldock and Rerank) [32] were combined in a multimodal (docking) and consensus (scoring) approach giving two sets of poses per ligand. The protocols share the same set of flexible residues: ALA154, ALA157, ALA164, ALA198, ALA201, ALA206, ARG195, ASN231, ASP148, ASP150, GLN214, GLU219, ILE202, ILE215, LEU217, LEU218, LYS165, MET98, MET103, MET155, MET161, MET199, MET232, PHE149, PHE97, PRO193, THR162, THR195, TRP160, TRP222, TYR158. Softened potentials were used with a tolerance of 1 and a strength 0.9. A search space volume of 17 Å radius was used around centered around and averaged position of known InhA ligands after structural alignment of proteins. The structural NAD molecule was treated as cofactor in calculations and was set as NAD+ with partial negative charges on phosphates and positive charge on aromatic nicotinamide group. Clustering of poses (tabu clustering) was set with an RMSD threshold of 1.9 Å. A simple template (pharmacophoric profile) was used with a strength of -500 and a grid resolution of 0.4 Å, other similarity measure parameters were let at their default values. This pharmacophoric profile uses two atoms: the oxygen of alcohol group from ligand JPL (3FNG PDB structure [27]) and the oxygen from the keto group of GEQ (1P44 PDB structure [13]). These atoms are representative of conserved hydrogen bond (donor/acceptors) positions involving oxygen atoms along InhA ligands.

In the case of OPT (Differential evolution algorithm) protocol, the docking process used 10000 iteration steps, and a grid resolution of 0.3 Å, along 40 independent runs. Internal parameters (population size, crossover rate, scaling factor ...) of the algorithm were let as default. A final minimization (per run) was parameterized using 4000 steps for lateral chains and 2000 steps for protein backbone preceded by a minimization and optimization (hydrogen bonds) of ligands. The same parameters were applied to the MSE (Simplex evolution algorithm) protocol, with 40 independent runs, internal parameters (population size, number of iterations, energy threshold...) of the algorithm were let as default. These protocols perform generally well with InhA structures, typical RMSD for reference ligands (i.e. TCL from 1P45 or JPL from 3FNG) were in the range of 0.5-1.0 Å for the best poses.

Pose topology analysis was carried on the best MolDock and Rerank scores. Conformity criterion was set as the ability to reproduce shared envelop of known ligand and typical interaction network: π-π or π-Alkyl interactions with nicotinamide group of NAD; hydrogen bonding with TYR158, hydrogen or electrostatic interactions with cofactor (OH from ribose, amido group, phosphates, charged nitrogen of pyridinium). In the context of consensus docking, if one or more poses combine the best values for each scoring scheme (Moldock and Rerank) they are described as strong poses.

### *4.4. Evaluation of InhA enzyme inhibition*

Kinetic assays were performed using *trans*-2-dodecenoyl-coenzyme A (DDCoA) and His6-InhA as previously described [9,33].

### *4.5. Minimal inhibitory concentration determination*

The drug susceptibility of MTB H37Rv strain was assessed using the resazurin microtiter assay (REMA), including positive and negative growth controls on each plate. Serial 2-fold dilutions of the compounds were made in a 96-well black plate (Fluoronuc, Thermo Fisher Scientific), followed by the addition of bacterial cultures in the log phase. After 7 days of incubation at 37 °C, 10 μL of resazurin (0.025% w/v) was added to each well, and fluorescence was measured after an additional overnight incubation using a Fluoroskan Microplate Fluorometer (Thermo Fisher Scientific; excitation = 544 nm; emission = 590 nm). Bacterial viability was determined as a percentage of resazurin turnover in the absence of the compound (internal negative control). Experiments were conducted in duplicate, and MIC90 values were obtained [34].

**Supplementary Materials:** The following supporting information can be downloaded. ($^{1}$H and $^{13}$C NMR spectra)

**Author Contributions:** "Conceptualization, CL; methodology, PH, JAD; FG and CL; validation, FR, GD, MRP and CL; formal analysis, PH, FG, AS; investigation, PH, FG, AS; resources, NSM, MRP, CL; data curation, FG, AS, CL; writing—original draft preparation, PH, FG, AS, NSM, FG, GD, MRP, CL; writing—review and editing, PH, AS, MRP, CL; visualization, FR, CL; supervision, GD, MRP, CL; project administration, CL; funding acquisition, CL . All authors have read and agreed to the published version of the manuscript."

**Funding:** This work was financially supported by the Centre National de la Recherche Scientifique (CNRS, France) and by Université Toulouse 3 Paul Sabatier (France).

**Acknowledgments:** We thank the mass spectrometry and chromatography services from the Institut de Chimie de Toulouse ICT-UAR 2599 (Université de Toulouse, CNRS, Toulouse, France, https://ict.cnrs.fr) for his help with chemical analyses.

**Conflicts of Interest:** "The authors declare no conflicts of interest."

## References


1. World Health Organization. Global Tuberculosis Report 2022; WHO: Geneva, 2021; pp 1–27.

2. Kakkar, A. K.; Dahiya, N. Bedaquiline for the treatment of resistant tuberculosis: Promises and Pitfalls. Tuberculosis 2014, 94, 357−362. DOI: 10.1016/j.tube.2014.04.001

3. Keam, S. J. Pretomanid: First approval. Drugs 2019, 79, 1797− 1803. DOI: 10.1007/s40265-019-01207-9

4. Ryan, N. J.; Lo, J. H. Delamanid: First global approval. Drugs 2014, 74, 1041−1045. DOI: 10.1007/s40265-014-0241-5

5. Boyne, M. E.; Sullivan, T. J.; amEnde C. W.; Lu, H.; Gruppo, V.; Heaslip, D.; Amin, A. G.; Chatterjee, D.; Lenaerts, A.; Tonge, P. J.; Slayden, R. A. Targeting fatty acid biosynthesis for the development of novel chemotherapeutics against Mycobacterium tuberculosis: evaluation of A-ring-modified diphenyl ethers as high-affinity InhA inhibitors. Antimicrob. Agents Chemother. 2007, 51, 3562–3567. DOI: 10.1128/AAC.00383-07

6. Pan, P.; Knudson, S.E.; Bommineni, G.; Li, H. J.; Lai, C. T.; Liu, N.; Garcia-Diaz, M.; Simmerling, C.; Patil, S. S., Slayden, R. A.; Tonge, P. J. Time-dependent diaryl ether inhibitors of InhA: structure-activity relationship studies of enzyme inhibition, antibacterial activity, and in vivo efficacy. ChemMedChem 2014, 9, 776–791. DOI: 10.1016/j.bioorg.2019.103498

7. Rodriguez, F.; Saffon, N.; Sammartino, J. C.; Degiacomi, G.; Pasca, M. R.; Lherbet, C. First triclosan-based macrocyclic inhibitors of InhA enzyme. Bioorg. Chem. 2020, 95, 103498. DOI: 10.1016/j.bioorg.2019.103498

8. Stec, J.; Vilcheze, C.; Lun, S.; Perryman, A. L.; Wang, X.; Freundlich, J.S.; Bishai, W.; Jacobs Jr., W. R.; Kozikowski, A. P. Biological evaluation of potent triclosan-derived inhibitors of the enoyl-acyl carrier protein reductase InhA in drug-sensitive and drug-resistant strains of Mycobacterium tuberculosis. ChemMedChem 2014, 9, 2528–2537. DOI: 10.1002/cmdc.201402255

9. Chebaiki, M.; Delfourne, E.; Tamhaev, R.; Danoun, S.; Rodriguez, F.; Hoffmann, P.; Grosjean, E.; Goncalves, F.; Azéma-Despeyroux, J.; Pál, A.; Korduláková, J.; Preuilh, N.; Britton, S.; Constant, P.; Marrakchi, H.; Maveyraud, L.; Mourey, L.; Lherbet, C. Discovery of new diaryl ether inhibitors against Mycobacterium tuberculosis targeting the minor portal of InhA. E. J. Med. Chem. 2023, 259, 115646. DOI: 10.1016/j.ejmech.2023.115646

10. Tamhaev, R.; Grosjean, E.; Ahamed, H.; Chebaiki, M.; Rodriguez, F.; Recchia, D.; Degiacomi, G.; Pasca, M. R.; Maveyraud, L.; Mourey, L.; Lherbet, C. Exploring the plasticity of the InhA substrate-binding site using new diaryl ether inhibitors. Bioorg. Chem. 2024, 143, 107032. DOI: 10.1016/j.bioorg.2023.107032

11. Shaikh, M.S.; Kanhed, A.M.; Chandrasekaran, B.; Palkar, M.B.; Agrawal, N.; Lherbet, C.; Hampannavar, G.A.; Karpoormath, R. Discovery of novel N-methyl carbazole tethered rhodanine derivatives as direct inhibitors of Mycobacterium tuberculosis InhA. Bioorg. Med. Chem. Lett. 2019, 29, 2338-2344. DOI: 10.1016/j.bmcl.2019.06.015

12. Chollet, A.; Mori, G.; Menendez, C.; Rodriguez, F.; Fabing, I.; Pasca, M. R.; Madacki, J.; Kordulakova, J.; Constant, P.; Quemard, A.; Bernardes-Genisson, V.; Lherbet, C.; Baltas, M. Design, synthesis and evaluation of new GEQ derivatives as inhibitors of InhA enzyme and Mycobacterium tuberculosis growth. Eur. J. Med. Chem. 2015, 101, 218–235. DOI: 10.1016/j.ejmech.2015.06.035

13. Kuo, M. R.; Morbidoni, H. R.; Alland, D.; Sneddon, S. F.; Gourlie, B. B.; Staveski, M. M.; Leonard, M.; Gregory, J. S.; Janjigian, A. D.; Yee, C.; Musser, J. M.; Kreiswirth, B.; Iwamoto, H.; Perozzo, R.; Jacobs Jr., W. R.; Sacchettini, J. C.; Fidock D. A. Targeting tuberculosis and malaria through inhibition of Enoyl reductase: compound activity and structural data. J. Biol. Chem. 2003, 278, 20851–20859. DOI: 10.1074/jbc.M211968200

14. Hartkoorn, R. C.; Sala, C.; Neres, J.; Pojer, F.; Magnet, S.; Mukherjee, R.; Uplekar, S.; Boy-Rottger, S.; Altmann, K. H.; Cole, S. T. Towards a new tuberculosis drug: pyridomycin - nature's isoniazid. EMBO Mol. Med. 2012, 4, 1032–1042. DOI: 10.1002/emmm.201201689

15. Kienle, M.; Eisenring, P.; Stoessel, B.; Horlacher, O. P.; Hasler, S.; van Colen, G.; Hartkoorn, R. C.; Vocat, A.; Cole, S. T.; Altmann, K.H. Synthesis and structure-activity relationship studies of C2-modified analogs of the antimycobacterial natural product pyridomycin. J. Med. Chem. 2020, 63, 1105–1131. DOI: 10.1021/acs.jmedchem.9b01457

16. Manjunatha, U. H.; Rao, S. P. S.; Kondreddi, R. R.; Noble, C. G.; Camacho, L. R.; Tan, B. H. Ng, S. H.; Ng, P. S.; Ma, N. L.; Lakshminarayana, S. B.; Herve, M.; Barnes, S. W.; Yu, W.; Kuhen, K.; Blasco, F.; Beer, D.; Walker; J. R.; Tonge, P. J.; Glynne, R.; Smith, P .W.; Diagana, T. T. Direct inhibitors of InhA are active against Mycobacterium tuberculosis. Sci. Transl. Med. 2015, 7, 269ra263. DOI: 10.1126/scitranslmed.3010597

17. Menendez, C.; Rodriguez, F.; Ribeiro, A. L.; Zara, F.; Frongia, C.; Lobjois, V.; Saffon, N.; Pasca, M. R.; Lherbet, C.; Baltas, M. Synthesis and evaluation of $\alpha$-ketotriazoles and $\alpha$,$\beta$-diketotriazoles as inhibitors of Mycobacterium tuberculosis. Eur. J. Med. Chem. 2013, 69, 167-173. DOI: 10.1016/j.ejmech.2013.06.042

18. Suresh, A.; Srinivasarao, S.; Agnieszka, N.; Ewa, A. K.; Alvala, M.; Lherbet, C.; Chandra Sekhar, K. V. G. Design and synthesis of 9H-fluorenone based 1,2,3-triazole analogues as Mycobacterium tuberculosis InhA inhibitors. Chem. Biol. Drug Des. 2018, 91, 1078–1086. DOI: 10.1111/cbdd.13127

19. Vau, D.; Krykun, S.; Pasca, M.R.; Frongia, C.; Lobjois, V.; Chassaing, S.; Lherbet, C.; Baltas, M. Triazolophthalazines - Easily accessible compounds with potent antitubercular activity. ChemMedChem. 2016, 11, 1078-1089. DOI: 10.1002/cmdc.201600085

20. Dumitrascu, F.; Georgescu, F.; Georgescu, E.; Caira, M. R. Pyrroloquinolines, imidazoquinolines, and pyrroloquinazolines with a bridgehead nitrogen. Adv. Het. Chem. 2019, 129, 155-244. doi:10.1016/bs.aihch.2019.01.004

21. Capelli, A.; Giuliani, G.; Anzini, M.; Riitano, D.; Giorgi, G.; Vomero, S. Design, synthesis, and structure-affinity relationship studies in NK1 receptor ligands based on azole-fused quinolinecarboxamide moieties. Bioorg. Med. Chem. 2008, 16, 6850-6859. DOI: 10.1016/j.bmc.2008.05.067

22. Cappelli, A.; Anzini, M.; Castriconi, F.; Grisci, G.; Paolino, M.; Braile, C.; Valenti, S.; Giuliani, G.; Vomero, S.; Di Capua, A.; Betti, L.; Giannaccini, G.; Lucacchini, A.; Ghelardini, C.; Di Cesare Mannelli, L.; Frosini, M.; Ricci, L.; Giorgi, G.; Mascia, M. P.; Biggio, G. Design, Synthesis, and Biological Evaluation of Imidazo[1,5-a]quinoline as Highly Potent Ligands of Central Benzodiazepine Receptors. J. Med. Chem. 2016, 59, 7, 3353-3372. DOI: 10.1021/acs.jmedchem.6b00034

23. Yan, Z.; Wan, C.; Yang, Y.; Zha, Z.; Wang, Z. The synthesis of imidazo[1,5-a]quinolones via a decarboxylative cyclization under metal-free conditions. RSC Adv. 2018, 8, 23058-23065. DOI: 10.1039/C8RA03786H

24. CCDC-2358967 (4g) and CCDC-2358968 (4h) contain the supplementary crystallographic data for this paper. These data can be obtained free of charge from The Cambridge Crystallographic Data Centre via https://www.ccdc.cam.ac.uk/structures/.]

25. Kondreddi, R. R.; Jiricek, J.; Rao, S. P. S.; Lakshminarayana, S. B.; Camacho, L. R.; Rao, R. ; Herve, M.; Bifani, P.; Ma, N. L.; Kuhen, K.; Goh, A.; Chatterjee, A. K.; Dick, T.; Diagana, T. T.; Manjunatha, U. H.; Smith, P. W. Design, synthesis, and biological evaluation of indole-2-carboxamides: a promising class of antituberculosis agents. J. Med. Chem. 2013, 56, 8849e8859. DOI: 10.1021/jm4012774

26. Franz, N. D.; Belardinelli, J. M.; Kaminski, M. A.; Dunn, L. C.; de Moura, V. C. N.; Blaha, M. A.; Truong, D. D.; Li, W.; Jackson, M.; North, E. J. Design, synthesis and evaluation of

indole-2-carboxamides with pan anti-mycobacterial activity. Bioorg. Med. Chem. 2017, 25, 3746e3755. DOI: 10.1016/j.bmc.2017.05.015

27. Freundlich, J.S.; Wang, F.; Vilcheze, C.; Gulten, G.; Langley, R.; Schiehser, G.A.; Jacobus, D.P.; Jacobs, W.R.; Sacchettini, J.C. Triclosan Derivatives: Towards Potent Inhibitors of Drug-Sensitive and Drug-Resistant Mycobacterium tuberculosis. ChemMedChem 2009, 4, 241-248. DOI: 10.1002/cmdc.200800261

28. Pettersen, E. F.; Goddard, T. D.; Huang, C. C.; Couch, G. S.; Greenblatt, D. M.; Meng, E. C.; Ferrin, T. E. J. UCSF Chimera - a visualization system for exploratory research and analysis. J. Comput. Chem. 2004, 25, 1605-1612. DOI: 10.1002/jcc.20084

29. Berman, H. M.; Westbrook, J.; Feng, Z.; Gilliland, G.; Bhat, T. N.; Weissig, N.; Shindyalov, I.; Bourne, P. E. The Protein Data Bank. Nucleic Acids Research 2000, 28, 235-242. DOI: 10.1093/nar/28.1.235

30. Meng, E. C.; Pettersen, E. F.; Couch, G. S.; Huang, C. C.; Ferrin, T. E. J. Tools for integrated sequence-structure analysis with UCSF Chimera. BMC Bioinformatics 2006, 7, 339-349. DOI: 10.1186/1471-2105-7-339

31. Rozwarski, D.A.; Vilchèze, C.; Sugantino, M.; Bittman, R.; Sacchettini, J.C. Crystal structure of the Mycobacterium tuberculosis enoyl-ACP reductase, InhA, in complex with NAD and a C16 fatty acyl substrate. J. Biol. Chem. 1999, 274, 15582-15589. DOI: 10.1074/jbc.274.22.15582

32. Thomsen, R.; Christensen, M. H. J. MolDock: a new technique for high-accuracy molecular docking. J. Med. Chem. 2006, 49, 3315-3321. DOI: 10.1021/jm051197e

33. Joshi, S. D.; Dixit, S. R.; Basha, J.; Kulkarni, V. H.; Aminabhavi, T. M.; Nadagouda, M. N.; Lherbet, C. Pharmacophore mapping, molecular docking, chemical synthesis of some novel pyrrolyl benzamide derivatives and evaluation of their inhibitory activity against enoyl-ACP reductase (InhA) and Mycobacterium tuberculosis. Bioorg. Chem. 2018, 81, 440-453. DOI: 10.1016/j.bioorg.2018.08.035

34. Degiacomi, G.; Gianibbi, B.; Recchia, D.; Stelitano, G.; Truglio, G. I.; Marra, P.; Stamilla, A.; Makarov, V.; Chiarelli, L. R.; Manetti, F.; Pasca, M. R. CanB, a druggable cellular target in Mycobacterium tuberculosis. ACS Omega 2023, 8, 25209-25220. DOI: 10.1021/acsomega.3c02311